

# First results from dark matter search experiment with LiF bolometer at Kamioka Underground Laboratory

K. Miuchi <sup>a,\*<sup>1</sup></sup>, M. Minowa <sup>a,b</sup>, A. Takeda <sup>a</sup>, H. Sekiya <sup>a</sup>,  
 Y. Shimizu <sup>a</sup>, Y. Inoue <sup>b,c</sup>, W. Ootani <sup>c</sup>, Y. Ootuka <sup>d</sup>

<sup>a</sup>*Department of Physics, School of Science, University of Tokyo, 7-3-1, Hongo,  
 Bunkyo-ku, Tokyo 113-0033, Japan*

<sup>b</sup>*Research Center for the Early Universe (RESCEU), School of Science, University  
 of Tokyo, 7-3-1, Hongo, Bunkyo-ku, Tokyo 113-0033 Japan*

<sup>c</sup>*International Center for Elementary Particle Physics (ICEPP), University of  
 Tokyo, 7-3-1, Hongo, Bunkyo-ku, Tokyo 113-0033 Japan*

<sup>d</sup>*Institute of Physics, University of Tsukuba, 1-1-1 Ten'nodai, Tsukuba, Ibaraki  
 305-8571, Japan*

---

## Abstract

Tokyo group has performed first underground dark matter search experiment in 2001 through 2002 at Kamioka Observatory (2700m.w.e). The detector is eight LiF bolometers with total mass 168g aiming for the direct detection of WIMPs via spin-dependent interaction. With a total exposure of 4.1 kg·days, we derived the limits in the  $a_p - a_n$  (WIMP-nucleon couplings) plane and excluded a large part of the parameter space allowed by the UKDMC experiment.

*Key words:* Dark matter, Neutralino WIMP, LiF, Bolometer

*PACS:* 14.80.Ly, 29.40.Ym, 95.35.+d

---

<sup>\*</sup> Corresponding author.

*Email address:* miuchi@icepp.s.u-tokyo.ac.jp (K. Miuchi).

<sup>1</sup> *Present Address:* Cosmic-Ray Group, Department of Physics, Faculty of Science, Kyoto University Kitashirakawa, Sakyo-ku, Kyoto, 606-8502, Japan

## 1 Introduction

Weakly Interacting Massive Particles (WIMPs) are thought to be the most promising dark matter candidates and many experiments have been performed for the direct detection of WIMPs. The DAMA experiment has reported to have detected WIMPs by an annual modulation signal with their 10kg NaI detectors[1]. The reported WIMP parameter region is  $M_{\text{WIMP}} = (52^{+10}_{-8})\text{GeVc}^{-2}$  and  $\sigma_{\text{WIMP-p}}^{\text{SI}} = (7.2^{+0.4}_{-0.9}) \cdot 10^{-6}\text{pb}$ . On the other hand, the CDMS Collaboration[2] and EDELWEISS Collaboration[3] reported to have excluded most of the parameter space claimed by the DAMA experiment. These experiments are aimed to detect WIMPs by the spin-independent interactions. In 2001, DAMA group published an paper interpreting the annual modulation signal in a spin-independent and spin-dependent mixed framework[12]. According to Ref. [12],  $\sigma_{\text{WIMP-p}}^{\text{SD}}$  could be as high as  $0.6\text{pb}$  for  $30 \sim 80\text{GeVc}^{-2}$  if we assume certain sets of parameters. These results suggest that WIMPs could be detected via spin-dependent interaction and dark matter search experiments should be performed both via spin-independent and spin-dependent interactions.

We, the Tokyo group, had developed a lithium fluoride (LiF) bolometer to detect WIMPs by the spin-dependent interaction in the surface laboratory[8] then performed pilot runs at shallow depth site[9]. We have improved our LiF bolometer since we installed the detector system in 2000 at Kamioka Observatory (2700m.w.e) and recently we made a dark matter search measurement in 2001 through 2002.

In this paper, we report our first results from the dark matter search experiment performed at Kamioka Observatory with a new limits in the  $a_p - a_n$  (WIMPs-nucleon couplings) plane.

## 2 Experimental set-up and measurements

The laboratory for this dark matter search experiment is newly caved near the Super-Kamiokande detector at Mozumi Mine of the Kamioka Mining and Smelting Co. located at Kamioka-cho, Gifu, Japan. The laboratory is at the depth of 2700 m.w.e and the muon flux is reduced about five orders of magnitude compared to the surface laboratory. As the radon concentration in the mine air is high and have a seasonal change (40 (winter)~1200 (summer) Bq/m<sup>3</sup>), the air is taken from the outside of the mine and is blown into the laboratory with a rate of 1 m<sup>3</sup>/min. The radon concentration in the room is less than 50 Bq/m<sup>3</sup>.

The detector for this dark matter search experiments is a LiF bolometer array consisting of eight LiF bolometers with a total mass of 168g. Each bolometer consists of a  $2 \times 2 \times 2$  cm $^3$  LiF crystal and a neutron transmutation doped (NTD) Ge thermistor ( $1.5 \times 1 \times 1$  mm $^3$ )[5] glued to the LiF with GE varnish. We refer to each bolometer as D1, D2,..., and D8. Four of the LiF crystals are purchased from BICRON Co. Ltd. (expressed as BIC in Table 1) while others are from OHYO KOKEN KOGYO Co. Ltd. (expressed as OKEN in Table 1). NTD3 thermistors, which have been used for most of the previous measurements, are used for the six of the eight bolometers, while NTD2 and NTD4 are used for one bolometer each. Characteristic of the NTD thermistors are shown in Ref. [5]. Radioactive contamination in the crystals are previously checked with a low-background Ge spectrometer and is found to be less than 0.2 ppb for U, 2 ppb for Th, and 20 ppm for K. Surfaces of the LiF crystals are etched with perchloric acid in order to eliminate remaining grains of the polishing powder. Features of the eight bolometers are summarized in Table 1.

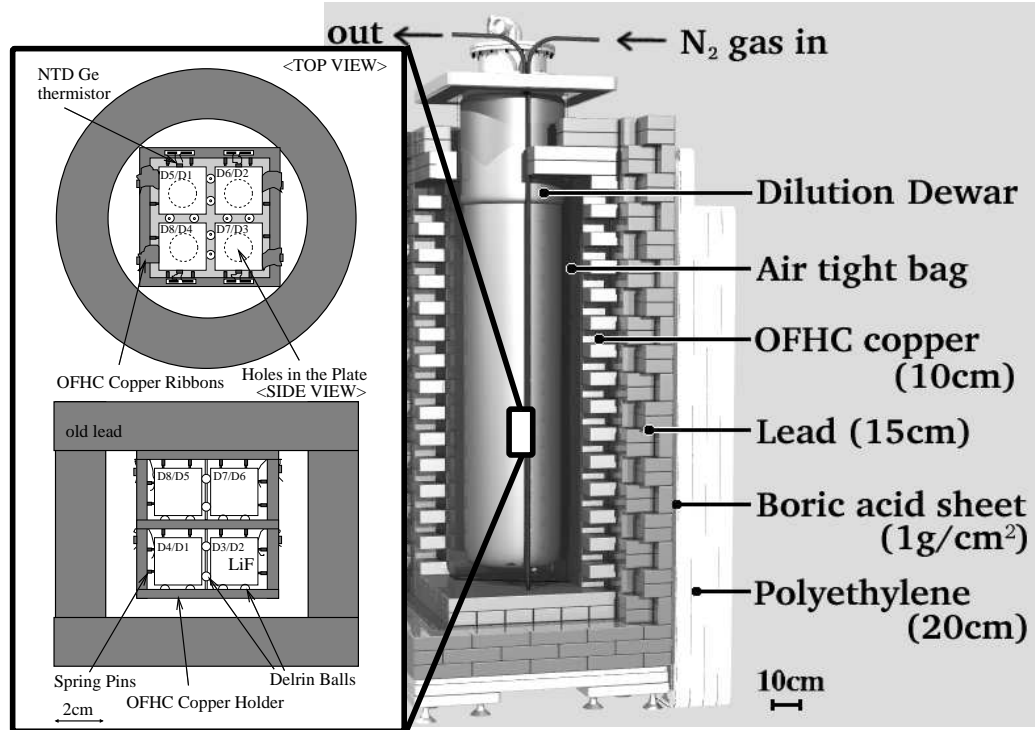


Fig. 1. Schematic drawings of the bolometer array.

Schematic drawing of the bolometer array is shown in Fig. 1. The array consists of two stages, each stage holding four bolometers. The bolometers are fixed with spring pins and Delrin balls. Thermal contacts between the LiF crystals

and the oxygen free high conductivity (OFHC) copper holder are achieved by annealed OFHC copper ribbons of 10 mm width and 0.1 mm thickness. The etching process and the assembly were performed in a clean bench of class 100. The bolometer array is encapsulated in a low radio-active lead (older than 200 years) of 2cm thickness. OFHC copper holder and inner shield are etched with nitric acid in order to eliminate the surface contamination.

Detector	D1	D2	D3	D4	D5	D6	D7	D8
mass (g)	20.98	20.98	20.99	20.92	21.09	21.07	21.01	21.00
LiF manufacturer	BIC	BIC	BIC	BIC	OKEN	OKEN	OKEN	OKEN
thermistor	NTD2	NTD3	NTD3	NTD3	NTD4	NTD3	NTD3	NTD3
Etching ( $\mu\text{m}$ )	21	22	26	29	22	24	27	30

Table 1

LiF bolometers used for this underground measurement. See the text.

The bolometer array and inner shields are suspended with three Kevlar cords from the bottom of the dilution refrigerator which is cooled down to below 10mK. The thermal connection to the dilution refrigerator is achieved by annealed four OFHC copper ribbons of 10 mm width, 120 mm length, and 0.1 mm thickness. Each Kevlar cord is 8 cm long and eliminates the microphonic noise due to the helium liquefier. The dilution refrigerator is constructed with the low radio-activity materials assayed with a low-background Ge spectrometer in advance.

The refrigerator is shielded with 10 cm of OFHC copper, 15cm of lead, 1g/cm<sup>2</sup> of boric acid sheet, and 20 cm of polyethylene as shown in Fig. 1. Materials for the passive shields are previously radio-assayed with a low-background Ge spectrometer[6]. An air tight plastic bag is set between the copper shield and the cryostat. The plastic bag is filled with nitrogen gas evaporated from the liquid nitrogen. The radon concentration is less than 0.2 Bq/m<sup>3</sup> throughout the measurement period, which makes negligible background to this dark matter search experiment.

Each thermistor is DC biased through a 300 M $\Omega$  load resistor. The bias current of each bolometer is listed in Table 2. The voltage change across the thermistor is fed to the voltage sensitive amplifier placed at the 4K cold stage. A junction field effect transistor (J-FET), NEC 2SK163 is used for the cold stage amplifier with a gain of 10. The signal from the cold stage amplifier is in turn amplified by the voltage amplifier placed at the room temperature with a gain of 4.86  $\times 10^2$ . The signal from the voltage amplifier undergoes through a low pass filter with a cut-off frequency of 11 Hz and is digitized with a sampling rate

of 1 kHz. All of the data are recorded continuously without any online trigger for a complete offline analysis. The data size for an hour measurement is 74M bytes.

The measurement is performed from November 22, 2001 through January 12, 2002. Eight of the bolometers worked, however, D1 and D5 have poor signal to noise ratio because of the thermistor (NTD2 and NTD4), and we analyzed the data taken by the other six bolometers.

We applied an offline level trigger to the data averaged over  $\pm 10$  msec. Trigger levels are determined so that the trigger rates do not exceed 1 Hz. The trigger levels and the trigger rates are shown in Table 2. We determined the energy of each event by fitting the scaled template signal to the raw data. Then the electric noise events and the events that are thought to have occurred within the thermistors are eliminated by the wave form analysis. Then the events above the threshold energy that is determined as the energy with efficiency=0.8 are selected as real bolometer signals. The trigger and event selection efficiencies are estimated by adding the scaled template signals to the raw data as described in Ref. [9]. Finally, the real bolometer events in coincidence with two or more detectors within  $\pm 10$  msec are discarded since WIMPs hardly interact in two or more detectors simultaneously. Energy resolutions of the bolometers are estimated by the same method as the efficiency estimation. The threshold energies used for the event selection and estimated energy resolution near the threshold are listed in Table 2.

The calibrations are carried out by irradiating  $^{60}\text{Co}$  and  $^{137}\text{Cs}$  gamma-ray sources suspended between the heavy shield and the cryogenics. Compton edges are used and good agreement with the simulations are seen. Good linearities are seen as shown in Ref. [9]. Linearities down to 60keV are confirmed previously[8]. Recorded pulse height to a given signal for six detectors are shown as 'gain' in Table 2. Gains are within the range of factor 7 which seems to be reasonable considering the assembly conditions are not exactly same for the six bolometers. The stability of the detector response and linearities are checked every three or four days and the gains are found to be stable within  $\pm 5\%$ .

### 3 Results

The spectra obtained with the six bolometers are shown in Fig. 2. One of the spectrum (D3) obtained in the pilot run at Nokogiriyama underground cell[9] is shown for comparison. Live times of the six bolometers are listed in Table 2. The total exposure is 4.1 kg·days. Background levels of D6, D7, and D8 have decreased by nearly one order of magnitude compared to the pilot run. D4

Detector	D2	D3	D4	D6	D7	D8
Bias Current[nA]	0.05	0.04	0.05	0.05	0.09	0.07
Gain[mV/keV]	0.62	1.1	2.1	1.2	0.38	2.5
Trigger level[mV]	8	8	15	6	3	5.5
Trigger rate [Hz]	0.15	0.12	0.57	0.011	0.35	0.14
Threshold [keV]	44.1	24.1	60.8	15.7	46.8	8.0
Event rate[ $10^{-3}$ Hz]	0.71	1.2	1.0	0.77	0.51	1.4
Resolution (FWHM)[keV]	13	8.0	10	3.5	7.8	1.9
Live Time[days]	33.2	33.4	30.1	34.3	31.7	33.3

Table 2

Detector responses of the six bolometers.

suffers from electronics noises, therefore the background level of D4 is higher than those of other detectors.

From the obtained spectra, we derived spin-dependent WIMP-proton elastic scattering cross section ( $\sigma_{\text{WIMP}-\text{p}}^{\text{SD}}$ ) limits. We calculated the limits in the same manner as used in Ref. [9] and Ref. [10].

Here we used the astrophysical and nuclear parameters listed in Table 3. We used the earth velocity which corresponds to the velocity in the measurement period. We used the  $\lambda^2 J(J+1)$  values calculated by assuming the odd group shell model[11]. For the WIMPs heavier than 50 GeV, the limits have been improved by factor 5 from the pilot run. Since we determined the energy threshold (efficiency=0.8) higher than the pilot run, we did not improve the cross section limits for the lighter WIMPs compared to the pilot run. The best limit is 23pb for  $M_{\text{WIMP}} = 40\text{GeV}$ .

Dark matter density	$\rho_D = 0.3\text{GeV}\text{c}^{-2}\text{cm}^{-3}$
Velocity distribution	Maxwellian
Maxwellian velocity parameter	$v_0 = 220\text{km}\text{s}^{-1}$
Escape velocity	$v_{\text{esc}} = 650\text{km}\text{s}^{-1}$
Earth velocity	$v_E = 217\text{km}\text{s}^{-1}$
spin factor( $^7\text{Li}$ )	$\lambda^2 J(J+1) = 0.411$
spin factor( $^{19}\text{F}$ )	$\lambda^2 J(J+1) = 0.647$

Table 3

Astrophysical and nuclear parameters used to derive the exclusion limit.

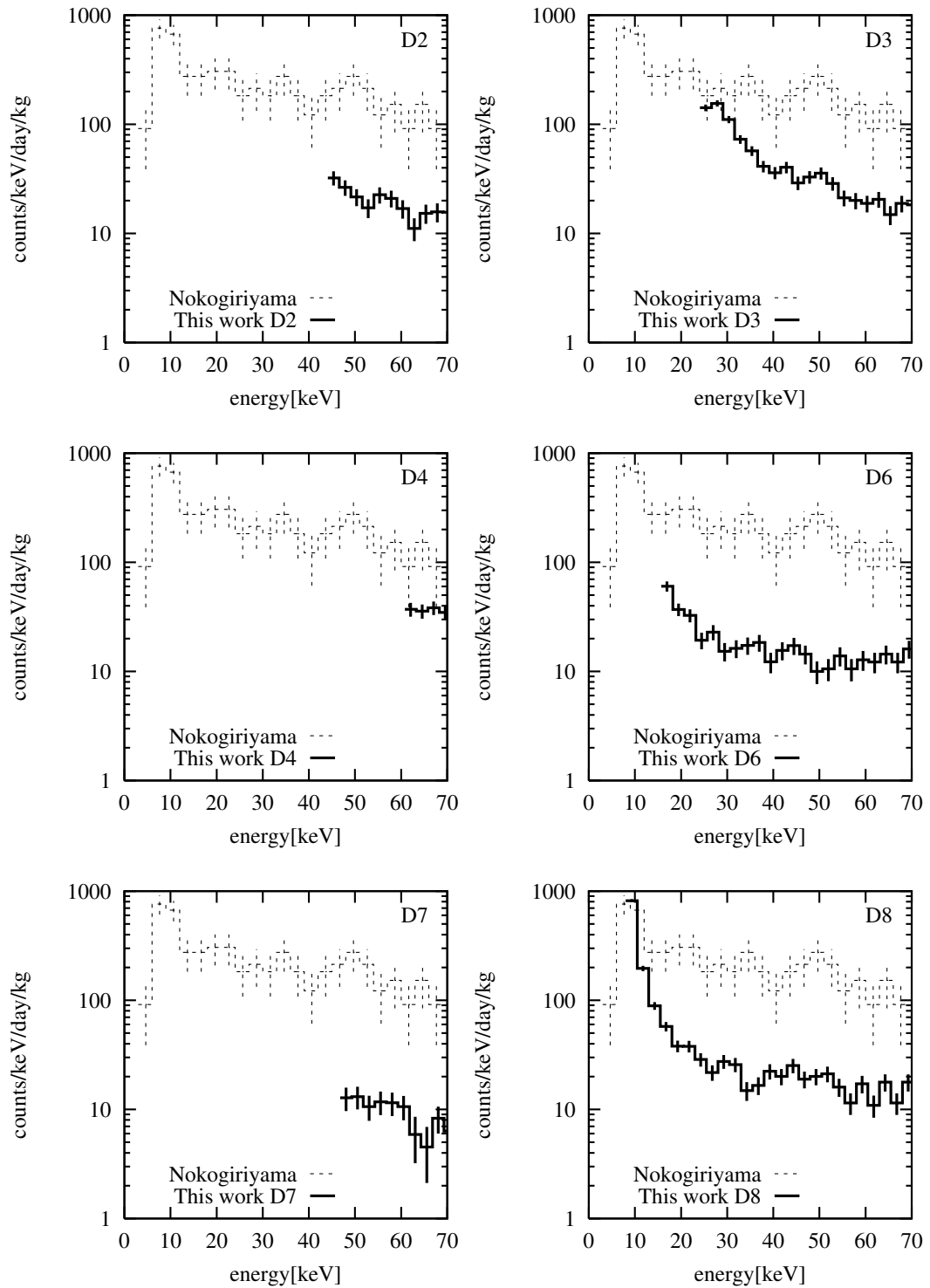


Fig. 2. Low energy spectra obtained with the six bolometers are shown in thick solid lines. Results from the pilot run(D3) is shown in dashed lines.

We also derived spin-dependent WIMP-proton and WIMP-neutron elastic scattering cross section limits from  ${}^7\text{Li}$  and  ${}^{19}\text{F}$  independently by the same manner as described in Ref. [7], or using

$$\sigma_{\text{WIMP}-\text{p(N)}}^{\text{SDlim}} = \sigma_{\text{WIMP}-\text{N}}^{\text{SDlim}} \frac{\mu_{\text{WIMP}-\text{p}}^2}{\mu_{\text{WIMP}-\text{N}}^2} \left( \frac{C_{\text{p(N)}}^{\text{SD}}}{C_{\text{p}}^{\text{SD}}} \right)^{-1} \quad (1)$$

and

$$\sigma_{\text{WIMP}-\text{n(N)}}^{\text{SDlim}} = \sigma_{\text{WIMP}-\text{N}}^{\text{SDlim}} \frac{\mu_{\text{WIMP}-\text{n}}^2}{\mu_{\text{WIMP}-\text{N}}^2} \left( \frac{C_{\text{n(N)}}^{\text{SD}}}{C_{\text{n}}^{\text{SD}}} \right)^{-1}, \quad (2)$$

where  $\sigma_{\text{WIMP}-\text{p(N)}}^{\text{SDlim}}$  and  $\sigma_{\text{WIMP}-\text{n(N)}}^{\text{SDlim}}$  are the spin-dependent WIMP-proton and WIMP-neutron cross section limits obtained with the assumptions that all events are due to WIMP-proton and WIMP-neutron elastic scatterings in the nucleus N, respectively,  $\sigma_{\text{WIMP}-\text{N}}^{\text{SDlim}}$  is the WIMP-nucleus cross section limit which is directly set by the experiments,  $\mu_{\text{WIMP}-\text{p}}$  and  $\mu_{\text{WIMP}-\text{n}}$  are the WIMP-proton and WIMP-neutron reduced masses, respectively,  $\mu_{\text{WIMP}-\text{N}}$  is the WIMP-nucleus reduced mass,  $C_{\text{p(N)}}^{\text{SD}}$  and  $C_{\text{n(N)}}^{\text{SD}}$  are the proton and neutron contributions to the total enhancement factor of nucleus N, respectively, and  $C_{\text{p}}^{\text{SD}}$  and  $C_{\text{n}}^{\text{SD}}$  are the enhancement factors of proton and neutron themselves, respectively. Ratios of the enhancement factors calculated by assuming the odd group shell model are shown in Table 4.

The enhancement factor and the cross section are related by the following equation:

$$\begin{aligned} \sigma_{\text{WIMP}-\text{N}}^{\text{SD}} &= 4G_F \mu_{\text{WIMP}-\text{N}}^2 C_{\text{N}}^{\text{SD}} \\ &= 4G_F^2 \mu_{\text{WIMP}-\text{N}}^2 \frac{8}{\pi} (a_{\text{p}} \langle S_{\text{p(N)}} \rangle + a_{\text{n}} \langle S_{\text{n(N)}} \rangle)^2 \frac{J+1}{J}, \end{aligned} \quad (3)$$

Isotopes	$J$	$\langle S_{\text{p(N)}} \rangle$	$\langle S_{\text{n(N)}} \rangle$	$C_{\text{p(N)}}^{\text{SD}}/C_{\text{p}}^{\text{SD}}$	$C_{\text{n(N)}}^{\text{SD}}/C_{\text{n}}^{\text{SD}}$
${}^7\text{Li}$	$3/2$	0.497	0.004	$5.49 \times 10^{-1}$	$3.56 \times 10^{-5}$
${}^{19}\text{F}$	$1/2$	0.441	-0.109	$7.78 \times 10^{-1}$	$4.75 \times 10^{-2}$
${}^{23}\text{Na}$	$3/2$	0.248	0.020	$1.37 \times 10^{-1}$	$8.89 \times 10^{-4}$
${}^{127}\text{I}$	$5/2$	0.309	0.075	$1.78 \times 10^{-1}$	$1.05 \times 10^{-2}$

Table 4

Values of  $\langle S_{\text{p(N)}} \rangle$ ,  $\langle S_{\text{n(N)}} \rangle$ ,  $C_{\text{p(N)}}^{\text{SD}}/C_{\text{p}}^{\text{SD}}$ ,  $C_{\text{n(N)}}^{\text{SD}}/C_{\text{n}}^{\text{SD}}$  for various isotopes. Values for  ${}^7\text{Li}$  and  ${}^{19}\text{F}$  are taken from Ref.[17] and those for  ${}^{23}\text{Na}$  and  ${}^{127}\text{I}$  are taken from Ref.[18]

where  $\sigma_{\text{WIMP-N}}^{\text{SD}}$  is the WIMP-nucleus cross section,  $G_F$  is the Fermi coupling constant,  $C_N^{\text{SD}}$  is total enhancement factor of nucleus N,  $a_p$  and  $a_n$  are the WIMP-proton and WIMP-neutron couplings, respectively,  $\langle S_{p(N)} \rangle$  and  $\langle S_{n(N)} \rangle$  are the expectation values of the proton and neutron spins within the nucleus N, respectively, and  $J$  is the total nuclear spin.  $\langle S_{p(N)} \rangle$ ,  $\langle S_{n(N)} \rangle$ , and  $J$  can be calculated with shell models and they are shown in Table 4.

From the obtained WIMP-proton and WIMP-neutron elastic scattering cross section limits, we derived the limits in the  $a_p - a_n$  plane. We again followed Ref. [7]. The allowed region in the  $a_p - a_n$  plane is defined as follows:

$$\left( \sqrt{\frac{a_p}{\sigma_{\text{WIMP-p(N)}}^{\text{SDlim}}}} \pm \sqrt{\frac{a_n}{\sigma_{\text{WIMP-n(N)}}^{\text{SDlim}}}} \right)^2 < \frac{\pi}{24G_F^2\mu_{\text{WIMP-p}}^2}, \quad (4)$$

where the relative sign inside the square is determined by the sign of  $\langle S_{p(N)} \rangle / \langle S_{n(N)} \rangle$ .

Obtained limits in the  $a_p - a_n$  plane for WIMPs with mass of 50 GeV are shown in Fig.4 (a). The regions between the two parallel lines are the allowed regions from  ${}^7\text{Li}$  and  ${}^{19}\text{F}$  alone, respectively. It is seen that single nuclide is not sufficient to set a finite limit in the  $a_p - a_n$  plane. As we have  ${}^7\text{Li}$  and  ${}^{19}\text{F}$  as the target, we can take the intersection of the two regions as the combined allowed region from the LiF detector. This is the merit of the detector consisting of more than two nuclides with sufficient spins. We show the allowed regions in the  $a_p - a_n$  plane obtained by this experiment for light WIMPs (Fig.4 (b)) and heavy WIMPs (Fig.4 (c)). The limits set by this experiment for  $M_{\text{WIMP}}=30\text{GeV}$  are  $|a_p| < 32$  and  $|a_p| < 133$ .

We compared our results with the results of other experiments. As DAMA group has not shown the results from  ${}^{23}\text{Na}$  and  ${}^{127}\text{I}$  independently[1,4,12], we were not able to compare our results with the spin-dependent annual modulation allowed regions suggested in Ref. [12]. Instead, we compared our results with the results from the UKDMC experiments[10,14]. Since UKDMC shows the limits from  ${}^{23}\text{Na}$  and  ${}^{127}\text{I}$  independently in Ref.[10] we can calculate the limits in the  $a_p - a_n$  from  ${}^{23}\text{Na}$  and  ${}^{127}\text{I}$  and combine the without any. As the exclusion limits from the UKDMC experiments are comparable to the DAMA's limits as shown in Fig. 3, we can show that our results would have possibly excluded some part of the DAMA's spin-dependent annual modulation allowed regions[12] in the  $a_p - a_n$  plane. It should be noted that limits in the  $a_p - a_n$  plane from the NaI detector are largely affected by the sensitivity ratio of  ${}^{23}\text{Na}$  and  ${}^{127}\text{I}$ ; the threshold of the detector and the quenching factor of  ${}^{127}\text{I}$  largely change the limits. Therefore, we did not take the risk of deriving the limits in the  $a_p - a_n$  from the experiments of which independent results from  ${}^{23}\text{Na}$  and  ${}^{127}\text{I}$  are not shown.

In Fig. 5, the allowed regions for the (a): sufficiently light WIMPs for which  $^{127}\text{I}$  loses the sensitivity and NaI effectively becomes a detector with one nuclide, (b): WIMPs with mass near the center value of DAMA’s annual modulation signal, and (c): WIMPs heavy enough for which  $^{23}\text{Na}$  and  $^{127}\text{I}$  both have good sensitivities, are shown. In the three plots, the limits from Na and I of UKDMC[10] are shown in dotted and dash-dotted lines, respectively, NaI combined limits of UKDMC[10] are shown in thin solid lines and LiF combined limits from this work are shown in thick solid lines. UKDMC published recalculated data[14] in which only NaI combined limit is shown, and we derived the limits in the  $a_p - a_n$  with an assumption that the the sensitivity ratios of  $^{23}\text{Na}$  and  $^{127}\text{I}$  are same as those shown in Ref. [10]. These new limits from Ref. [14] are shown in dashed lines just for reference.

It is seen that our results can set limits complementary to the results obtained with NaI detectors. For the light WIMPs (lighter than 20 GeV for most of the detectors) for which  $^{127}\text{I}$  loses sensitivity, this is the only experiment that can set finite allowed region in the  $a_p - a_n$  plane. For the WIMPs with mass of 50 GeV, we exclude more than two thirds of the parameter space allowed by the UKDMC experiments. For the WIMPs with mass of 100 GeV, we only exclude a part of the UKDMC allowed region, however, it must be stressed that though our  $\sigma_{\text{WIMP}-p}^{\text{SD}}$  limits are about two orders of magnitude worse than the limits of UKDMC as shown in Fig. 3 , we are able to tighten their limits in the  $a_p - a_n$  plane. This is because the spin factors of  $^{19}\text{F}$  is large and the  $\langle S_{p(N)} \rangle / \langle S_{n(N)} \rangle$  sign of  $^{19}\text{F}$  is different from those of  $^7\text{Li}$ ,  $^{23}\text{Na}$ , and  $^{127}\text{I}$ .

#### 4 Discussions and prospects

Though we are able to tighten the limits from the UKDMC experiment in the  $a_p - a_n$  plane, the background is still high for the direct detection of WIMPs. We studied the background sources and found that potassium contamination on the surface of the LiF crystals, tritium produced by the neutron capture of  $^6\text{Li}$  during the development in the surface laboratory, and the uranium and thorium contamination in the OFHC copper holder and in the inner lead shield dominate the background in the energy region between 10 keV and 90 keV. We are planning to etch the LiF crystals more deeply in order to eliminate the contamination on the surface of the LiF crystals. We also plan to use NaF crystals as a bolometer in order to eliminate the effect of the tritium. It is also expected that NaF crystals give more stringent limits in the  $a_p - a_n$  plane since  $^{19}\text{F}$  and  $^{23}\text{Na}$  set limits orthogonal to each other in the  $a_p - a_n$  plane as shown in Fig. 4 and Fig. 5. We are planning to install active shields between the LiF crystals and the OFHC copper holders to reduce the background from the OFHC copper holder and the inner shield. With these improvements, we expect to improve the sensitivity of our detector by more than one order of

magnitude.

## 5 Conclusions

We have performed first underground dark matter experiment at Kamioka Observatory. With a total exposure of 4.1 kg·days, we have obtained  $\sigma_{\text{WIMP-p}}^{\text{SD}}$  limits factor 5 improved from the pilot run at Nokogiriyama underground cell. We calculated the limits in the  $a_p - a_n$  plane and showed that our results tightened the limits from the UKDMC experiment. For the WIMPs with mass of 50 GeV, we have excluded more than two thirds of the parameter space in the  $a_p - a_n$  plane allowed by the UKDMC experiment.

## Acknowledgements

We thank all the staffs of Kamioka Observatory of the Institute for Cosmic Ray Research, University of Tokyo for their hospitality in using the facilities of the Observatory. We want to express our gratitude to Prof. Komura at Kanazawa University for providing us with 25kg of low-activity old lead. This research is supported by the Grant-in-Aid for COE Research by the Japanese Ministry of Education, Culture, Sports, Science and Technology.

## References

- [1] R. Bernabei et al., Phys. Lett. B **424**(1998)195, R .Bernabei et al., Phys. Lett. B **450**(1999)448, and R. Bernabei et al., Phys. Lett. B **480**(2000)23.
- [2] CDMS Collaboration, Phys. Rev. Lett. **84**(2000)5699.
- [3] EDELWEISS Collaboration, Phys. Lett. B **513**(2001)15.
- [4] R. Bernabei et al., Phys. Lett. B **389**(1996)757.
- [5] W. Ootani et al., Nucl. Instr. Meth. A **372**(1996)534.
- [6] K. Miuchi, master thesis, University of Tokyo, 1999.
- [7] D.R. Tovey, R.J. Gaitskell, P. Gondolo, Y. Ramachers, L. Roszkowski, Phys. Lett. B **488**(2000)17.
- [8] W. Ootani et al., Astroparticle Physics **9**(1998)325.
- [9] W. Ootani et al.,Phys. Lett. B **461**(1999)371, and W. Ootani et al., Nucl. Instr. Meth. A **436**(1999)233.

- [10] P.F. Smith et al., Phys. Lett. B **379**(1996)299.
- [11] J. Ellis and R. A. Flores, Nucl. Phys. B**400**(1993)25.
- [12] R. Bernabei et al., Phys. Lett. B **509**(2001)197.
- [13] J.D. Lewin and P.F. Smith, Astroparticle Physics **6**(1996)87.
- [14] N.J.C. Spooner et al., Phys. Lett. B **473**(2000)330.
- [15] P.Belli et al., Nucl. Phys. B **563**(1999)97.
- [16] J.I. Collar, J. Puibasset, T.A. Girard, D. Limagne, H.S. Miley, and G. Waysand, Phys. Rev. Lett. **85**(2000)3083.
- [17] A. F. Pacheco and D. Strottman Phys. Rev. D **40**(1989)2131.
- [18] M.T. Ressell and D.J. Dean, Phys. Rev. C **56**(1997)535.

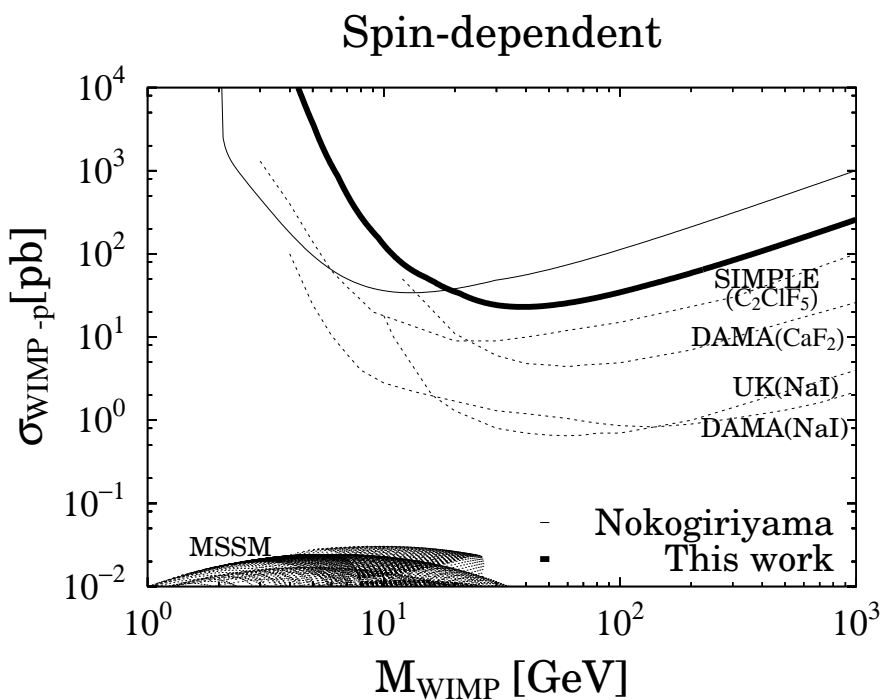


Fig. 3. 90% C.L.  $\sigma_{\text{WIMP}-\text{p}}^{\text{SD}}$  limit as a function of  $M_{\text{WIMP}}$  is shown in thick solid line. Results from pilot run(thin solid line), results from other experiments(dotted lines)[4,14–16], and MSSM predictions are also shown.

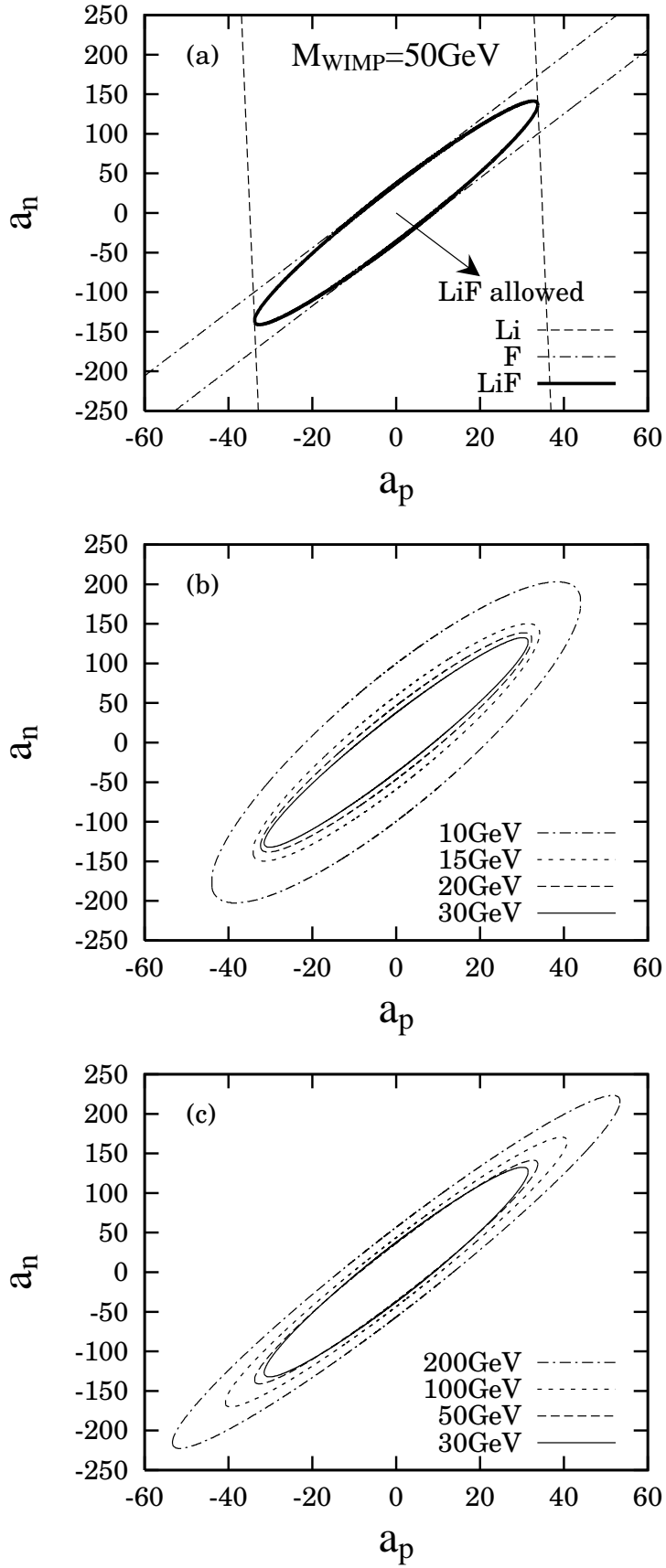


Fig. 4. Limits in the  $a_p - a_n$  plane.: (a) For  $M_{\text{WIMP}} = 50\text{GeV}$ , limits set by Li(F) alone are shown in dashed(dash-dotted) lines whiles the combined limits are shown in solid lines. (b) Limits for the light WIMPs. (c) Limits for the heavy WIMPs.

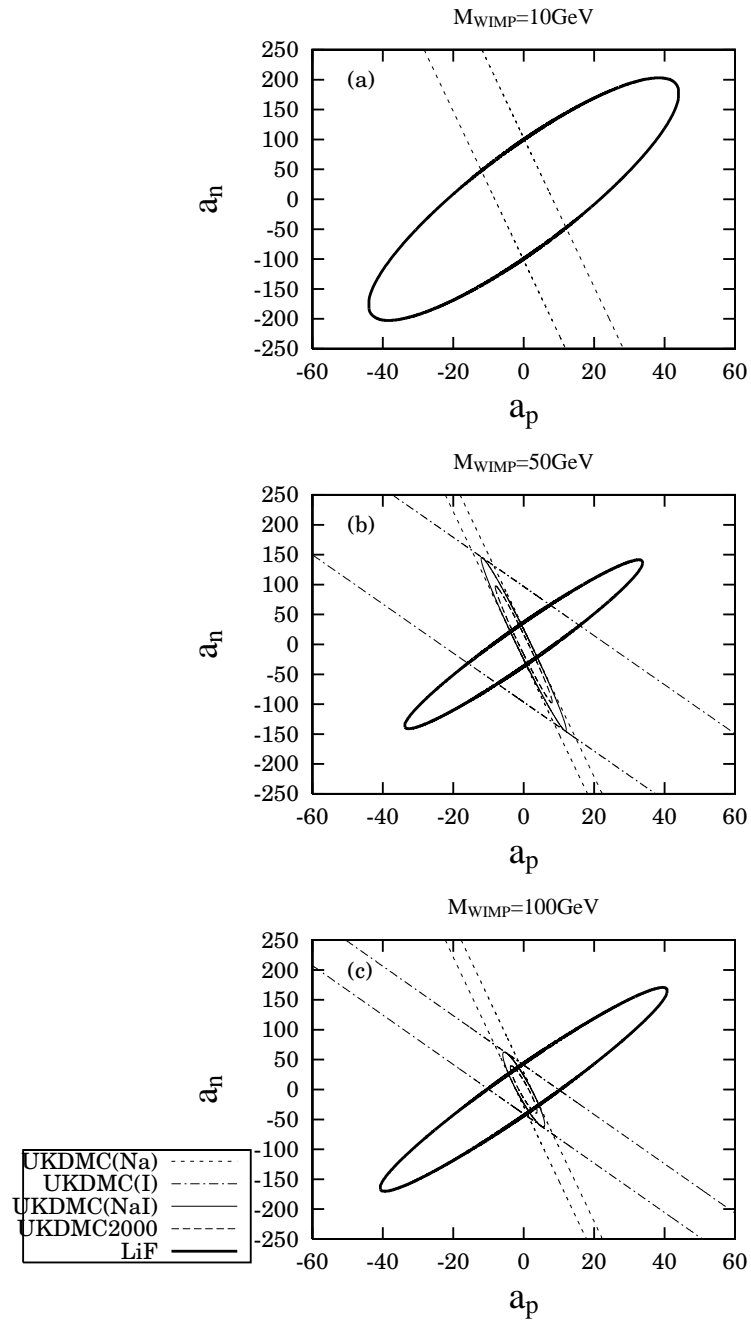


Fig. 5. Comparison of the limits in the  $a_p - a_n$  plane with the UKDMC data[10] for various WIMPs masses.